Supporting Information

High activity nitrogen-doped hollow carbon/silicon hollow spheres as encapsulated Pd-Fe nanoreactors for acetylene dialkoxycarbonylation

Fusheng Huang [a], Yongkang Sun [a], Jichang Liu [a] , Bin Dai [a,*], Jiangbing Li [a,*], Xuhong Guo [a,b,*]

[a] School of Chemistry and Chemical Engineering/State Key Laboratory Incubation Base for Green Processing of Chemical Engineering, Shihezi University, Shihezi 832003, China. E-mail: 20202007061@stu.shzu.edu.cn (Fusheng Huang), 20212307309@stu.shzu.edu.cn (Yongkang Sun), liujc@ecust.edu.cn (Jichang Liu), db_tea@shzu.edu.cn (Bin Dai), ljbing@126.com (Jiangbing Li), guoxuhong@ecust.edu.cn (Xuhong Guo)

[b] School of Chemical Engineering, East China University of Science and Technology, Shanghai 200237, China. E-mail: guoxuhong@ecust.edu.cn

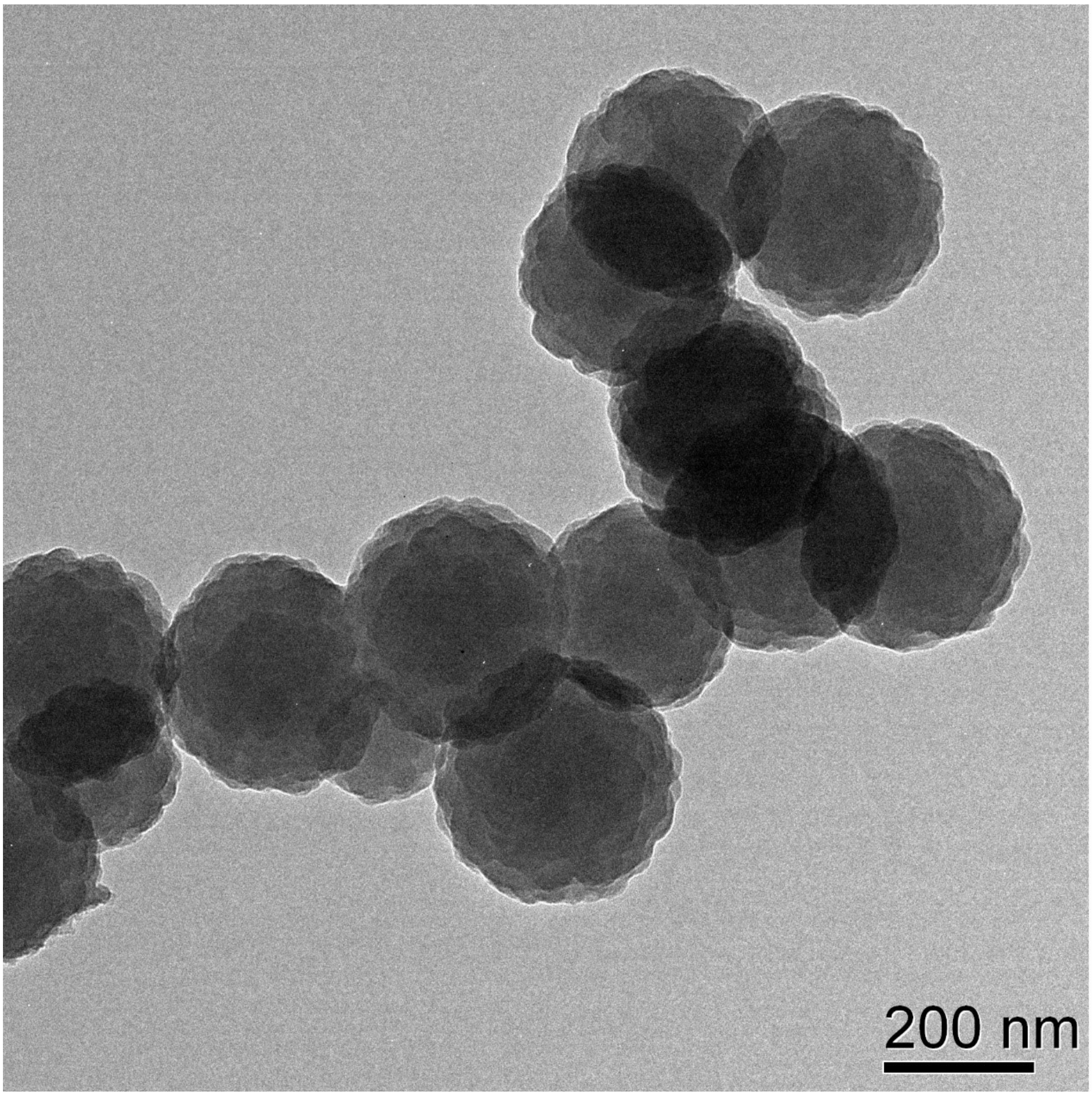

Figure S1 TEM image of PB@mSiO_2

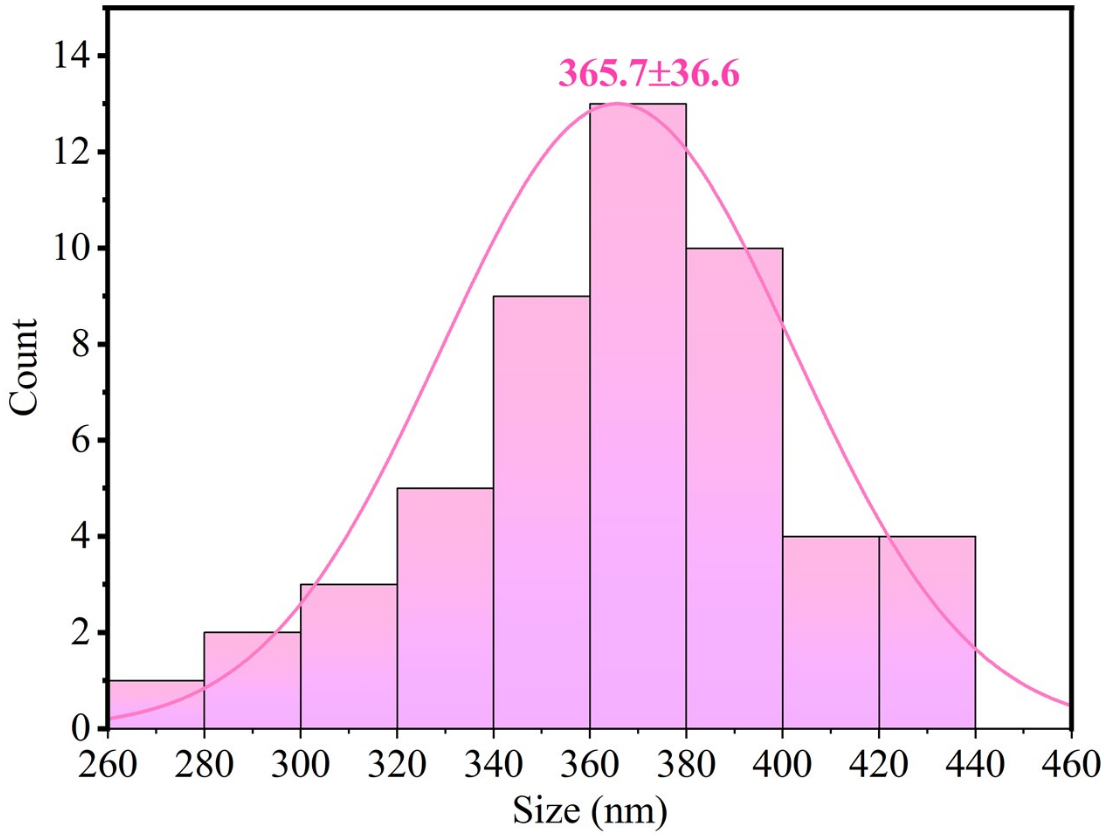

Figure S2. Histogram of particle size of PB@mSiO_2 nanoparticles

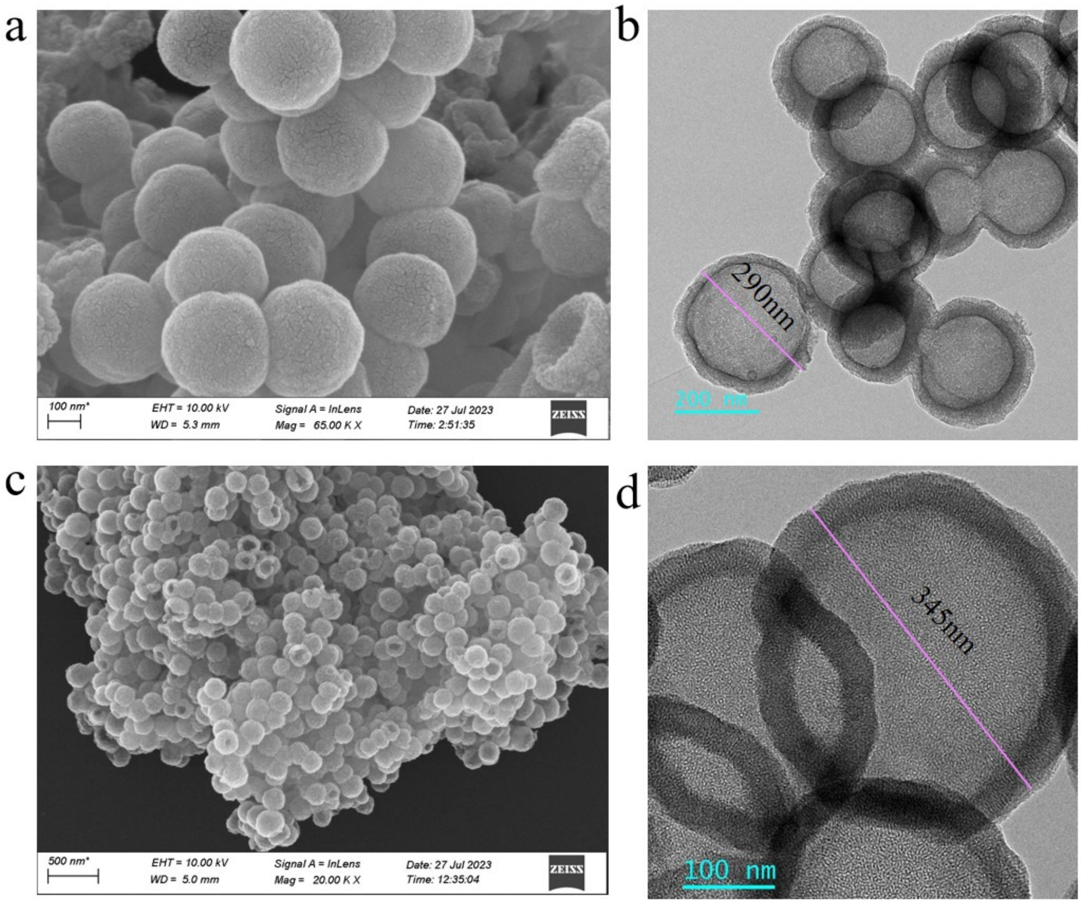

Figure S3. SEM (a) and TEM (b) images of the N_xC hollow spheres, SEM (c) and TEM (d) images of the $mSiO_2$ hollow spheres.

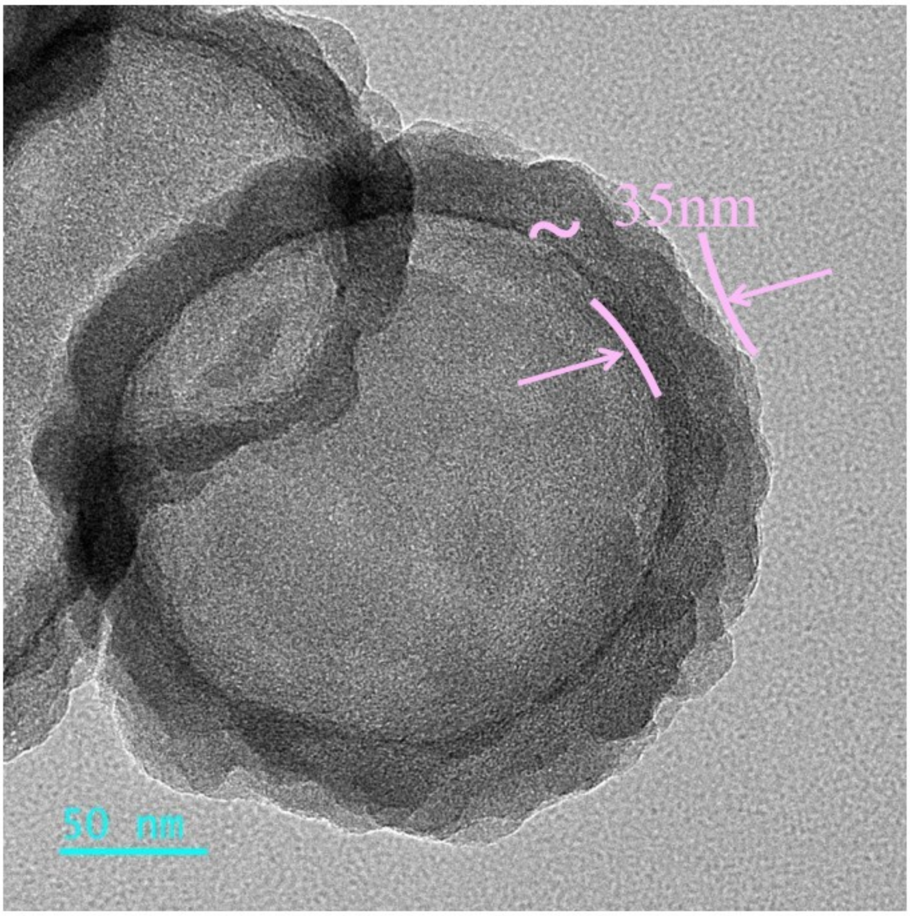

Figure S4. HAADF-STEM image of $N_xC@mSiO_2$ hollow spheres.

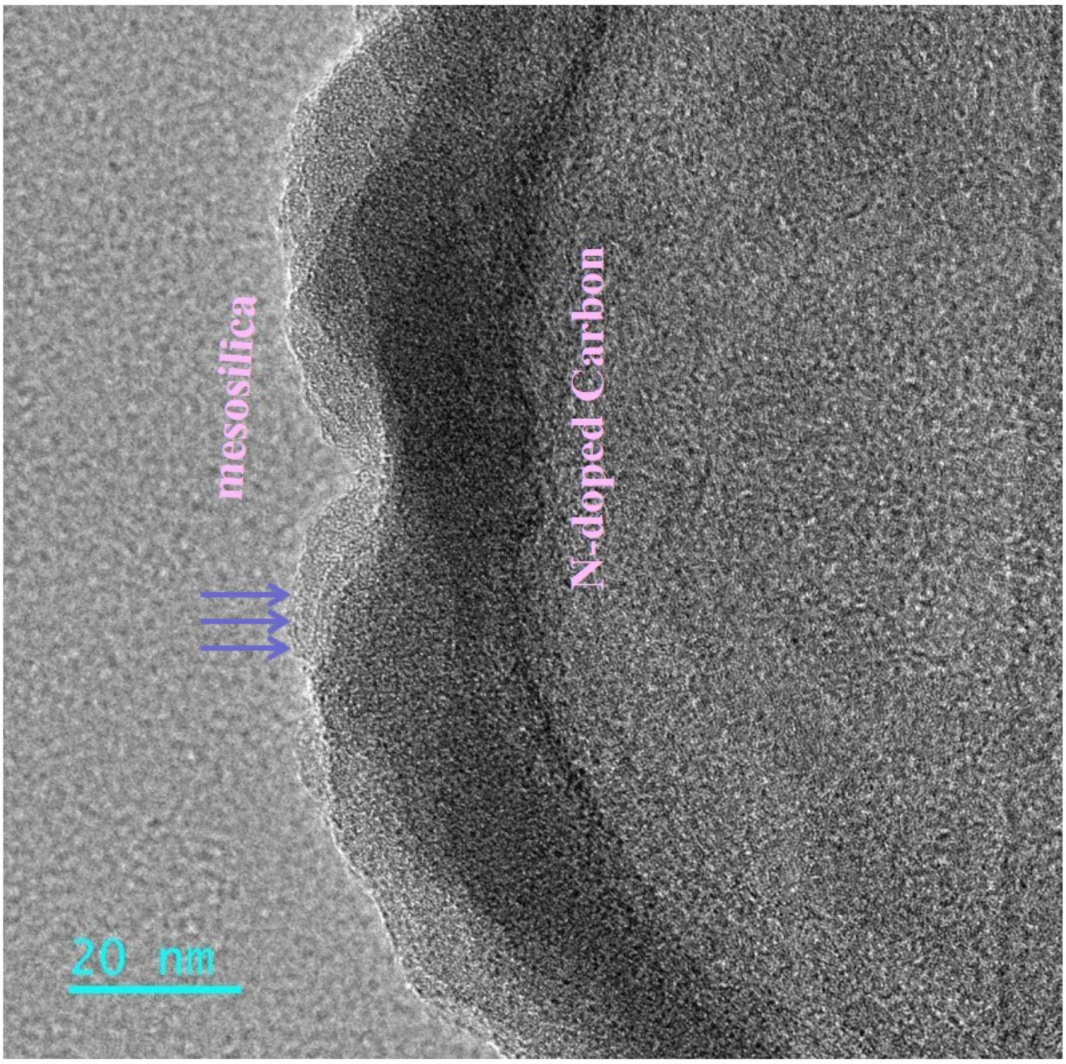

Figure S5.TEM images of $N_xC@mSiO_2$ hollow spheres.

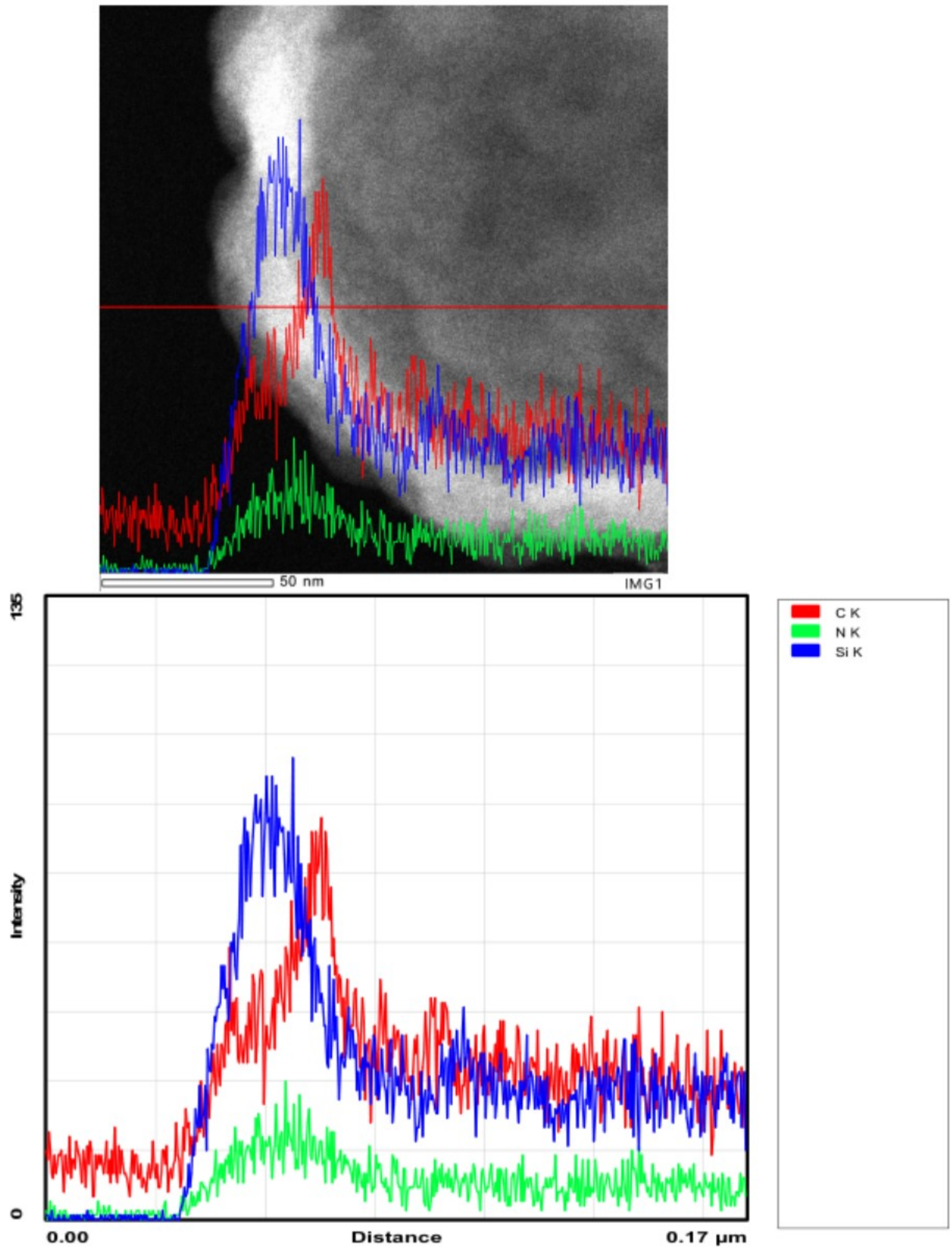

Figure S6. TEM line-scan image of $N_xC@mSiO_2$ hollow spheres.

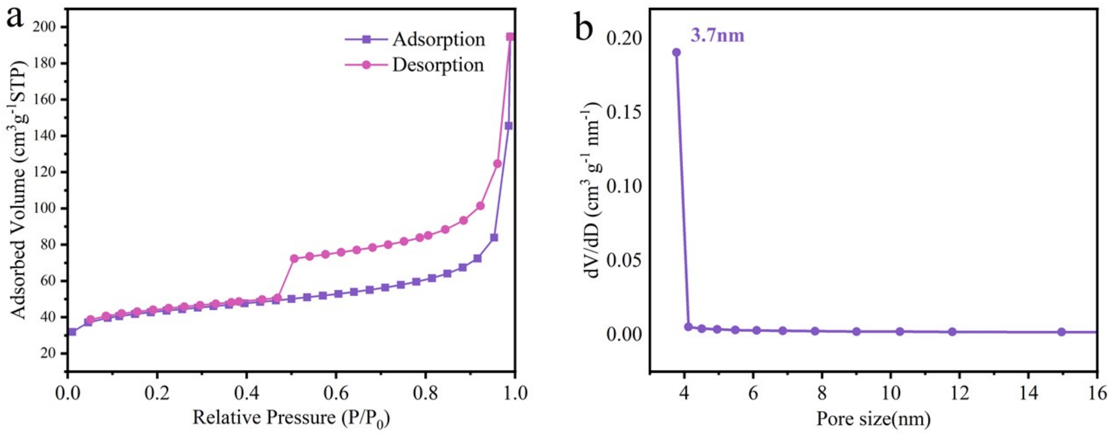

Figure S7. Nitrogen adsorption-desorption isotherm (a) and pore size distribution (b) of the N_xC@mSiO_2 hollow spheres.

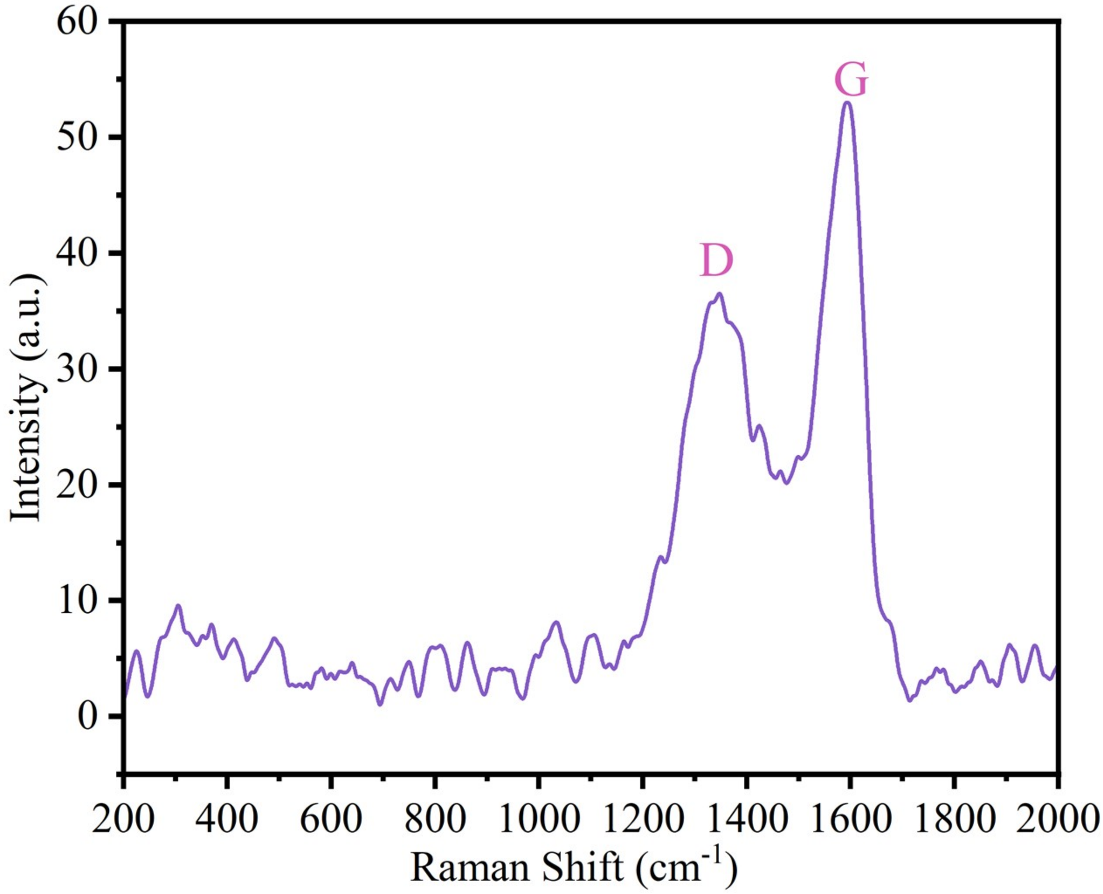

Figure S8. Raman spectrum of $N_xC@mSiO_2$ hollow spheres.

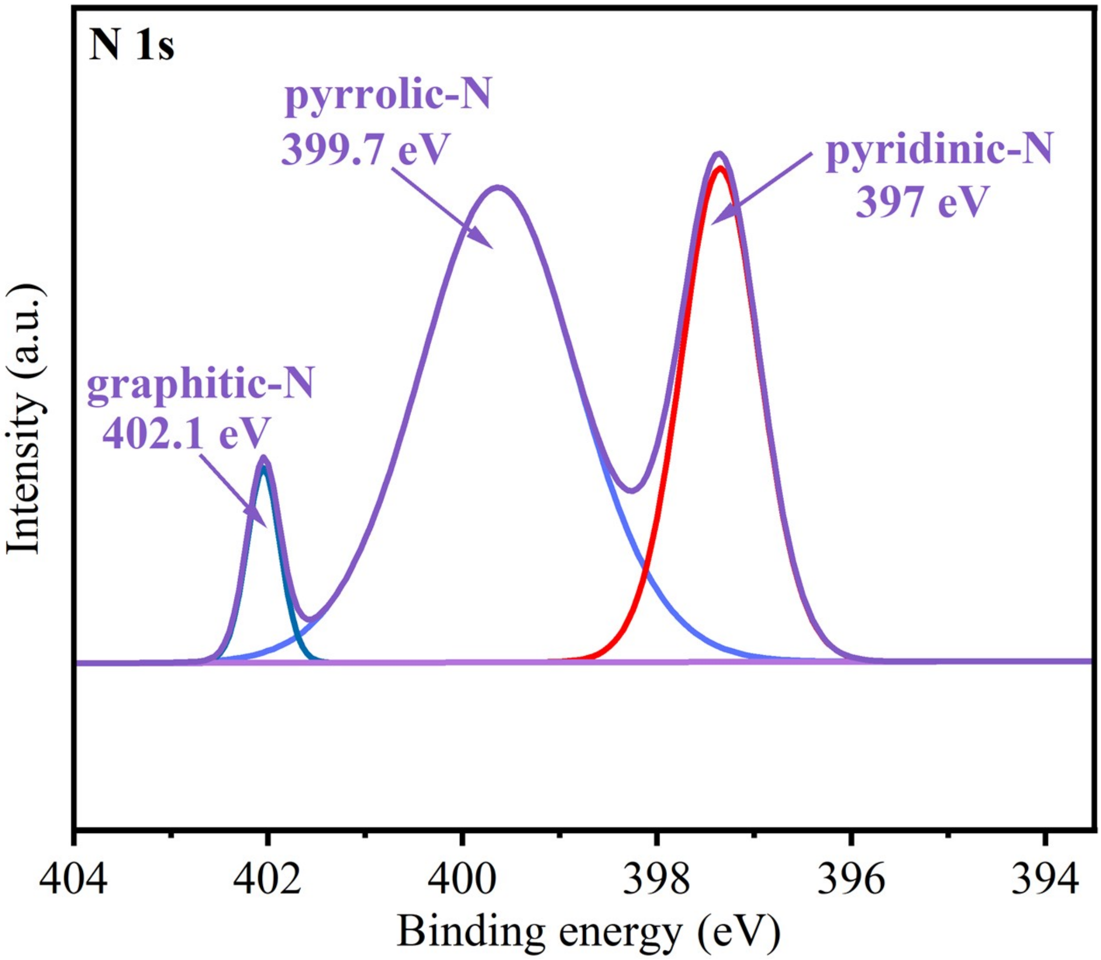

Figure S9. N 1s XPS spectrum of $N_xC@mSiO_2$ hollow spheres.

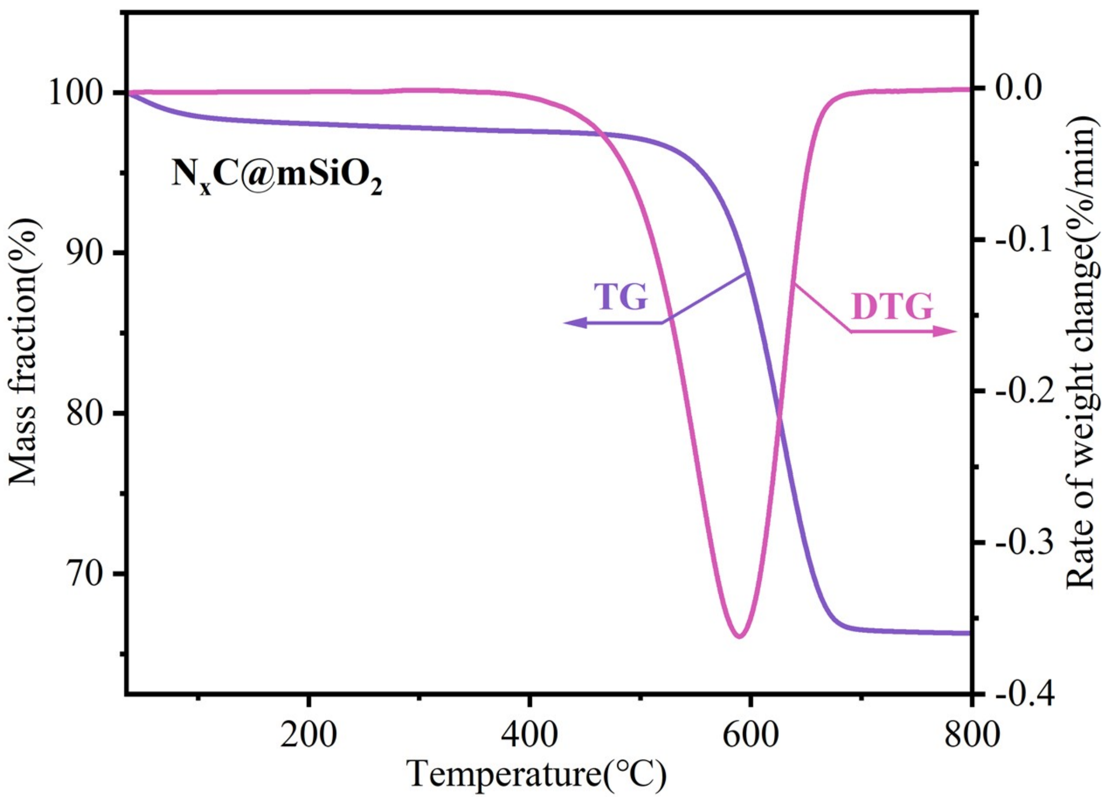

Figure S10. TG and DTG curves of $N_xC@mSiO_2$ obtained at air atmosphere.

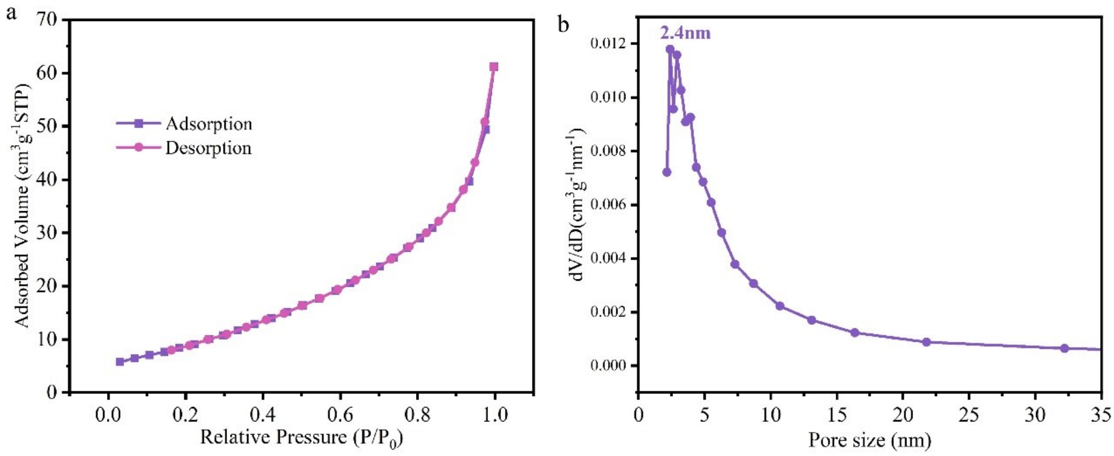

Figure S11. $Pd_4Fe_1/N_xC@mSiO_2$ Nitrogen adsorption-desorption isotherm and pore size distribution of hollow spheres.

Table S1 The specific surface area and pore structure of the synthesized sample

Entry	Samples	S_{BET}[a] (m^2/g)	V_t[b] (cm^3/g)
1	$N_xC@mSiO_2$	187	0.157
2	$Pd_4Fe_1/N_xC@mSiO_2$	36	0.088

[a]Specific surface area (S_{BET}) was calculated by using the BET method. [b]Total pore volume (V_{total}) was obtained at $p/p_0 = 0.990$.

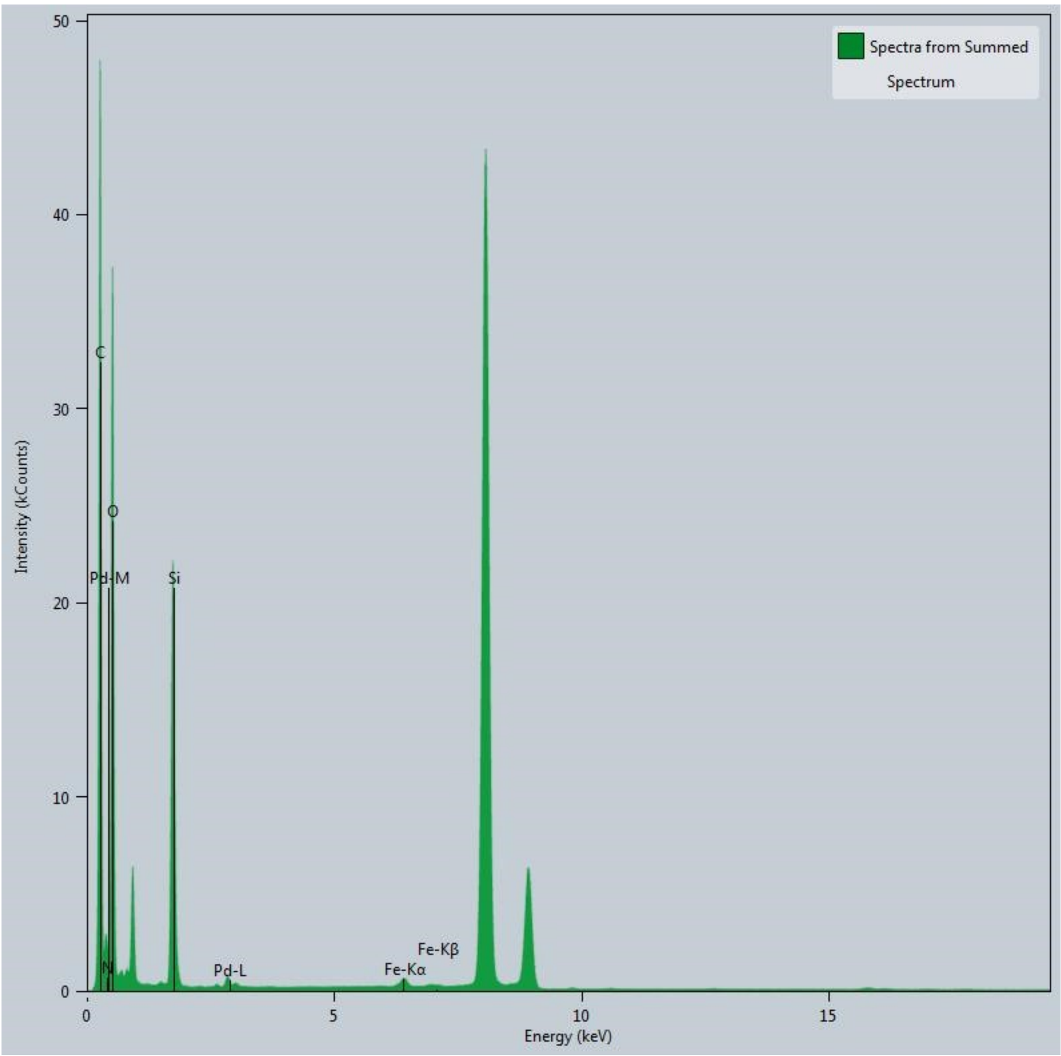

Figure S12. EDX image of catalyst $Pd_4Fe_1/N_xC@mSiO_2$

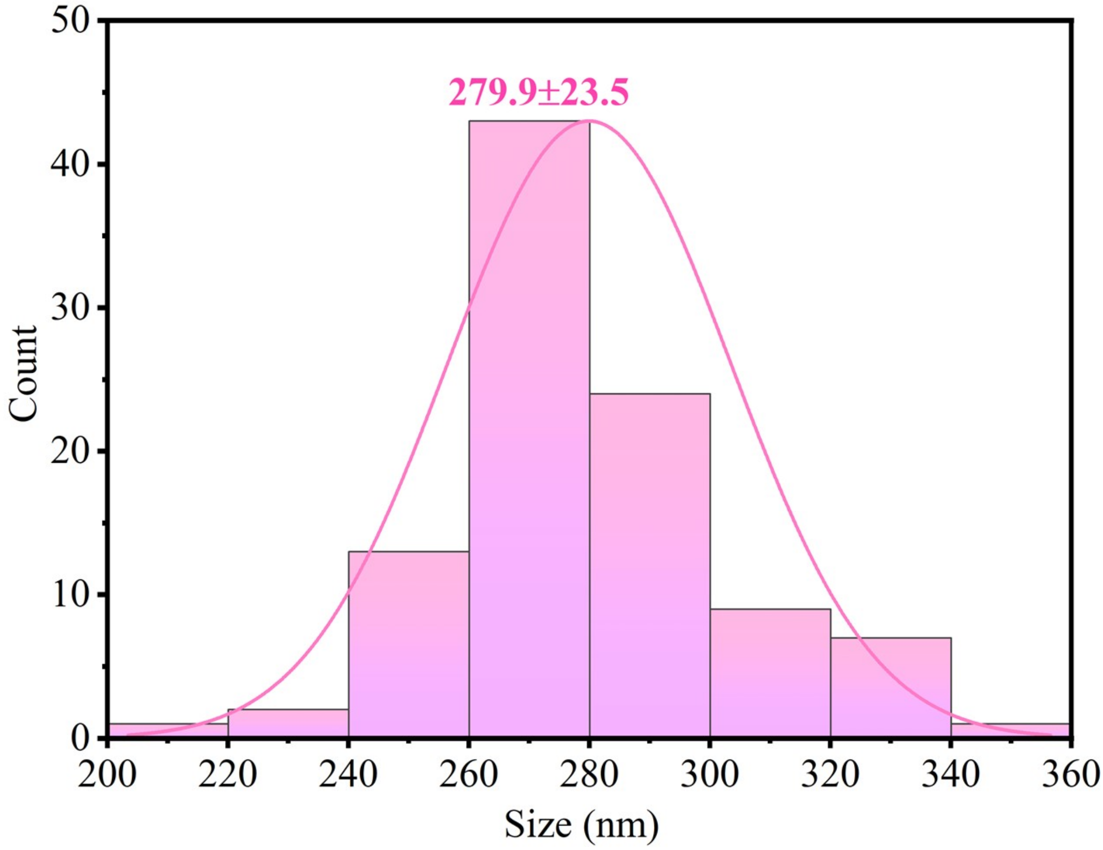

Figure S13. Histogram of particle size of $Pd_4Fe_1N_xC@mSiO_2$ nanoparticles

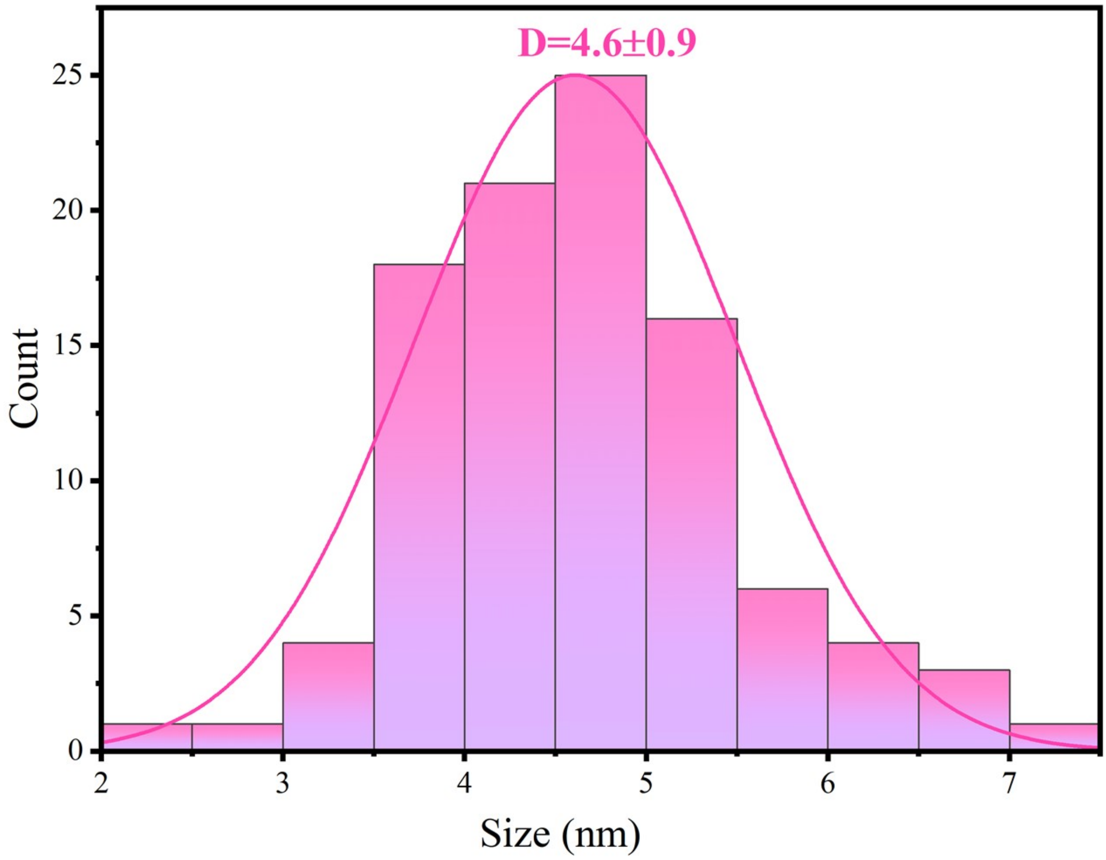

Figure S14. $Pd_4Fe_1/N_xC@mSiO_2$ Metal particle size distribution histogram of catalyst.

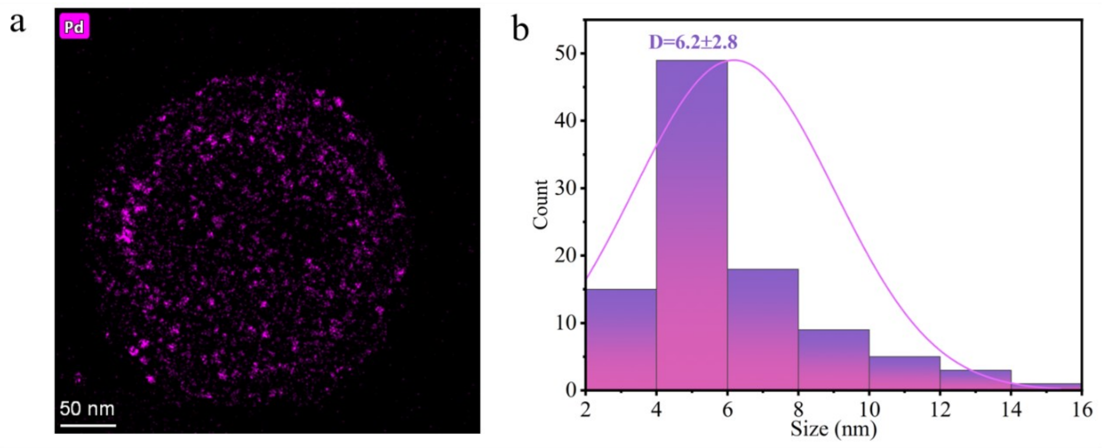

Figure S15.mpping diagram (a) and particle size distribution diagram (b) of catalyst Pd $Pd_5/N_xC@mSiO_2$

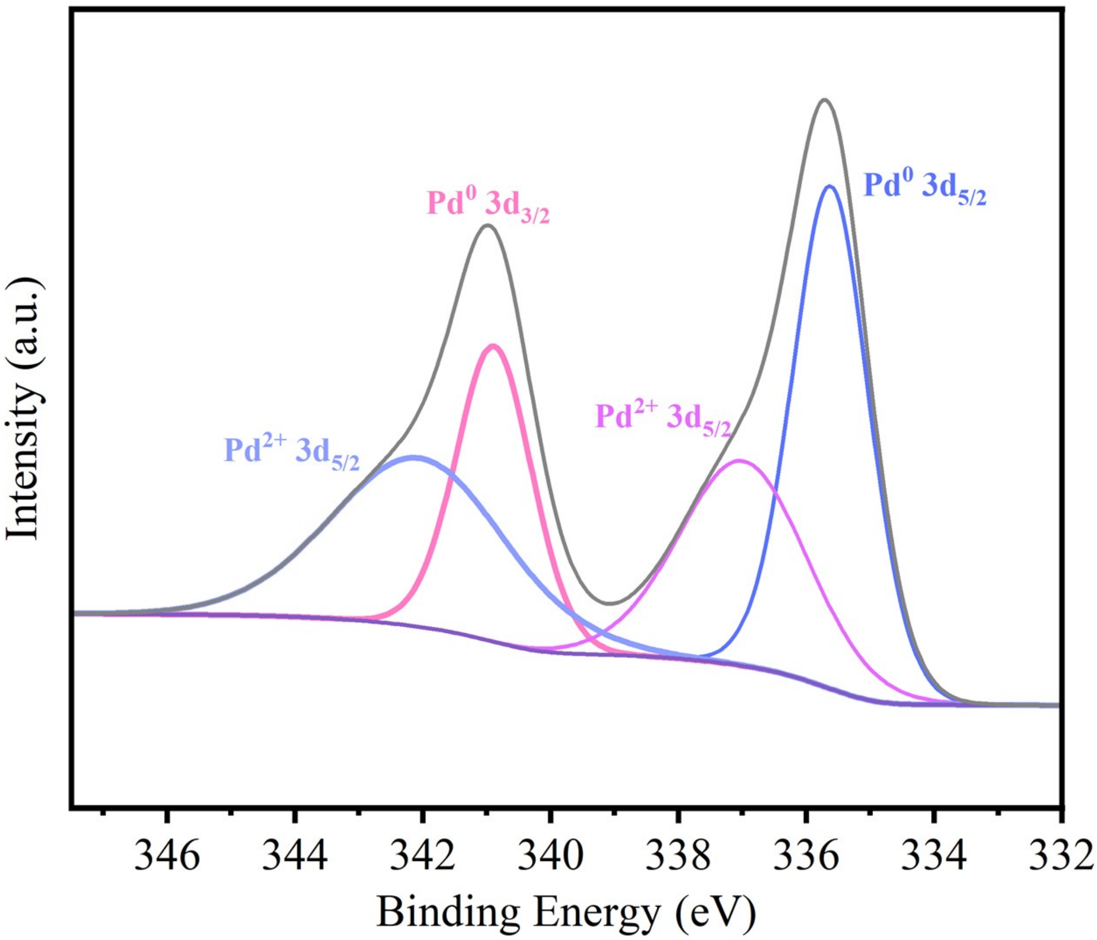

Figure S16. Pd 3d XPS spectrum of $Pd_5/N_xC@mSiO_2$ hollow spheres.

Table S2. XRD comparison of different catalysts

	Pd	Fe
Sample	atom %	atom %
$Pd_4Fe_{0.5}/N_xC@mSiO_2$	84.2	15.8
$Pd_4Fe_1/N_xC@mSiO_2$	68.7	31.3
$Pd_4Fe_2N_xC@mSiO_2$	62.3	37.7
$Pd_4Fe_3/N_xC@mSiO_2$	56.6	43.4

Table S3. XPS comparison of different catalysts

	Pd	Fe
Sample	atom %	atom %
$Pd_4Fe_{0.5}/N_xC@mSiO_2$	84.7	15.3
$Pd_4Fe_1/N_xC@mSiO_2$	68.6	31.4
$Pd_4Fe_2N_xC@mSiO_2$	61.3	38.7
$Pd_4Fe_3/N_xC@mSiO_2$	51.3	48.7

Table S4. Surface state of the catalysts from XPS

sample	Pd^0		Pd^{2+}		Fe^{2+}	
	$3d_{5/2}$	$3d_{3/2}$	$3d_{5/2}$	$3d_{3/2}$	$2p_{3/2}$	$2p_{1/2}$
$Pd_5/N_xC@mSiO_2$	335.6	340.9	337	342	-	-
$Pd_4Fe_{0.5}/N_xC@mSiO_2$	335.81	341.11	337.24	342.5	710.17	722.74
$Pd_4Fe_1/N_xC@mSiO_2$	335.95	341.23	337.4	342.96	709.83	722.81
$Pd_4Fe_2/N_xC@mSiO_2$	336.04	341.35	337.27	342.55	710.02	723.18
$Pd_4Fe_3/N_xC@mSiO_2$	336.11	341.38	337.19	342.37	710.12	723.12

Table S5. Element proportions corresponding to XPS peaks of different catalysts

	Pd^0	Pd^{2+}	Fe^{3+}	Fe^2
Sample	atom %	atom %	atom %	atom %
$Pd_4Fe_{0.5}/N_xC@mSiO_2$	72.42	27.58	67.35	32.65
$Pd_4Fe_1/N_xC@mSiO_2$	73.3	26.7	65.4	34.6
$Pd_4Fe_2N_xC@mSiO_2$	68.62	31.38	76.82	23.18
$Pd_4Fe_3/N_xC@mSiO_2$	65.46	34.54	73.18	26.82

Table S6. Comparison of catalytic properties of catalysts prepared with different carriers for acetylene dialkoxycarbonylation.

Catalyst	Conv. (%)	Sel. (%)		
		EA	DESu	DMM+DMF
Pd_4Fe_1/N_xC	86.1	---	---	80.4
Pd_4Fe_1/C	82.7	---	---	76.4
$Pd_4Fe_1/mSiO_2$	75.6	---	---	52.1

Reaction conditions: catalyst 0.05 g, acetylene (11 mmol), CH_3OH (20 mL), P_{CO} = 3.4 MPa, P_{air} = 1.6 MPa, 343K. The Conv.% is the acetylene conversion and the Sel.% is the selectivity of alkyne dialkoxycarbonylation, including DESu, DEM and DEF. EA, DESu, DEM, DEF denote ethyl acrylate, diethyl succinate, diethyl maleate (Z) and diethyl fumarate (E), respectively.

Table S7. Reaction time effect on the catalytic activity of $Pd_4Fe_1/N_xC@mSiO_2$ catalyst for acetylene dialkoxycarbonylation.

		Sel. (%)		
T (h)	Conv. (%)	EA	DESu	DMM+DMF
1	75.6	---	---	53.4
2	80.8			72.8
3	85.8	---	---	80.7
4	88.4			83.5
5	90.6	---	---	85.6

Reaction conditions: catalyst (0.05 g $Pd_4Fe_1/N_xC@mSiO_2$), acetylene (11 mmol), CH_3OH (20 mL), P_{CO} = 3.4 MPa, P_{air} = 1.6 MPa, 343K. The Conv.% is the acetylene conversion and the Sel.% is the selectivity of alkyne dialkoxycarbonylation, including DESu, DEM and DEF. EA, DESu, DEM, DEF denote ethyl acrylate, diethyl succinate, diethyl maleate (Z) and diethyl fumarate (E), respectively.

Table S8. Temperature effect on the catalytic activity of $Pd_4Fe_1/N_xC@mSiO_2$ catalyst for acetylene dialkoxycarbonylation.

				Sel. (%)
T (k)	Conv. (%)	EA	DESu	DMM+DMF
313	65.4			60.6
323	77.8	---	---	72.1
333	83.6	---	---	78.6
343	90.2	---	---	85.4
353	91.4			86.2

Reaction conditions: catalyst (0.05 g $Pd_4Fe_1/N_xC@mSiO_2$), acetylene (11 mmol), CH_3OH (20 mL), P_{CO} = 3.4 MPa, P_{air} = 1.6 MPa, 5.0 h. The Conv.% is the acetylene conversion and the Sel.% is the selectivity of alkyne dialkoxycarbonylation, including DESu, DEM and DEF. EA, DESu, DEM, DEF denote ethyl acrylate, diethyl succinate, diethyl maleate (Z) and diethyl fumarate (E), respectively.

Table S9. ICP test is used for Pd and Fe content in acetylene dialkoxycarbonylation $Pd_4Fe_1/N_xC@mSiO_2$.

Samples	Pd loading	Fe loading
Fresh $Pd_4Fe_1/N_xC@mSiO_2$	3.67	0.78
Spent $Pd_4Fe_1/N_xC@mSiO_2$	3.32	0.64

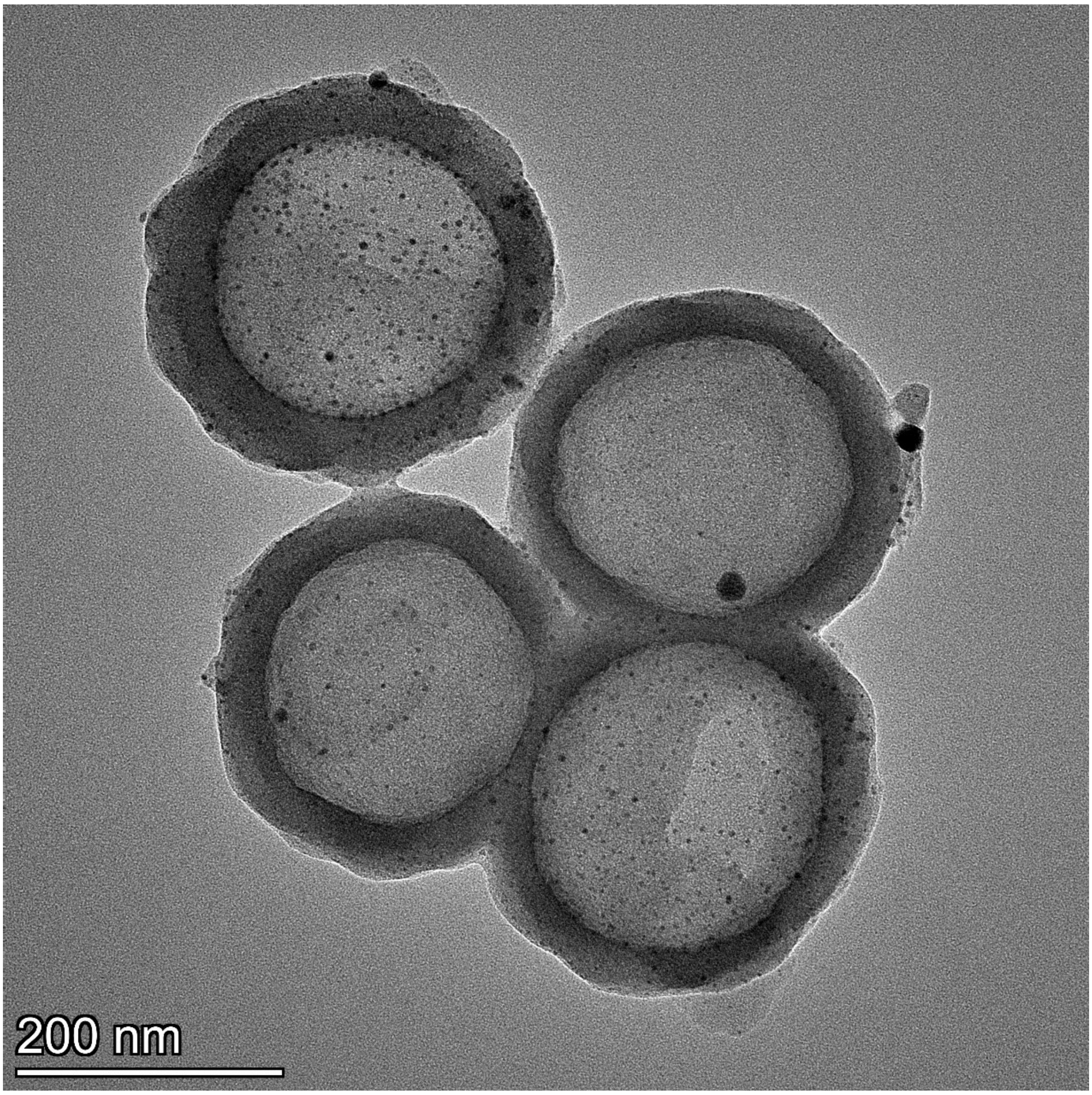

Figure S17. $Pd_4Fe_1/N_xC@mSiO_2$ TEM with five cycles

Table S7. Comparison of catalytic performance among different catalysts in acetylene dialkoxycarbonylation

entry	Catalyst	Conv.(%)	Sel.(%) MA	Sel.(%) DMSu	Sel.(%) DMM+DMF	reference
1	[a]$Pd_4Fe_1/N_xC@mSiO_2$	90.2	-	-	85.4	**This work**
2	[a]$Pd/N_xC@mSiO_2$	90	-	-	85	1
3	[a]Pd/N_xC	85.1	-	-	78.4	1
4	[a]$Pd/mSiO_2$	75.3	-	-	55.7	1
5	[a]Pd/MCM-41	65.1	-	-	45.61	1
6	[a]$Pd/C@mSiO_2$	78.9	-	-	70.49	1
7	[b]Pd_1/PIP_s	53.3	0	6.3	93.7	2
8	[b]Pd/NaY	0	0	0	0	2
9	[b]Pd/AC	0	0	0	0	2
10	[c]$Pd/g\text{-}C_3N_4$	trace	0	0	0	3
11	[c]Pd/SiO_2	12.6	0	-	49.4	3
12	[c]Pd/CeO_2	8.0	0	-	100	3
13	[c]Pd/Al_2O_3	10.2	0	-	100	3
14	[c]Pd/AC	21.9	0	-	100	3
15	[c]Pd/AC(nanosheet)	43.8	0	-	100	3
16	[d]Pd/Fe_2O_3+KI	80	0	-	78	4
17	[e]Homo.Pd+Cu	86	-	-	100	5

Reaction conditions: [a]catalyst (0.05 g, 4 wt.% Pd, 1 wt.% Fe), acetylene (11.0 mmol), CH_3OH (20 mL), P_{CO} = 3.4 MPa, P_{air} = 1.6 MPa, 343K, 5.0 h. [b]Reference.[1] Catalyst (0.3 g Pd/PIPs, 1 wt % Pd;0.3 g Pd/ NaY, 1 wt % Pd; 0.3 g Pd/AC, 1 wt % Pd), acetylene (9.0 mmol), CH_3OH (10.0 g), P_d = 2.2 MPa, Pair = 3.0 MPa, 373 K, 3.0 h). [c]Reference.[2] T = 353 K; 0.05 g catalyst; P_{CO} = 4.55 MPa; PO_2= 0.45 MPa; t =10h. [d]Reference.[3] T = 353 K, 0.05 g catalyst, 10 mmol of C_2H_2, O_2 + CO (1:10, 5MPa), and KI as a promoter for 5 h. [e]Reference.[4] Conv. (%) is the conversion of acetylene, MA denotes methyl acrylate, and sel. (%) is 1,4dicarboxylic acid esters including DMSu, DMM, and DMF.

Reference：

[1] Huang F, Sun Y, Liu J, et al. Nitrogen-oxygen co-doped carbon@silica hollow spheres as encapsulated Pd nanoreactors for acetylene dialkoxycarbonylation[J]. Journal of Colloid and Interface Science 662 (2024) 479-489.

[2] X. Li, S. Feng, P. Hemberger, A. Bodi, X. Song, Q. Yuan, J. Mu, B. Li, Z. Jiang, Y. Ding, Iodide-Coordinated Single-Site Pd Catalysts for Alkyne Dialkoxycarbonylation, ACS Catalysis 11 (2021) 9242-9251.

[3] X. Wei, Z. Ma, J. Lu, X. Mu, B. Hu, The highly efficient and selective dicarbonylation of acetylene catalysed by palladium nanosheets supported on activated carbon, New Journal of Chemistry 44 (2020) 11835-11840.

[4] X. Wei, Z. Ma, J. Lu, X. Mu, B. Hu, Strong metal-support interactions between palladium nanoclusters and hematite toward enhanced acetylene dicarbonylation at low temperature, New Journal of Chemistry 44 (2020) 1221-1227.

[5] C. Yang, K. Li, J. Wang, S. Zhou, Selective hydrogenation of phenol to cyclohexanone over Pd nanoparticles encaged hollow mesoporous silica catalytic nanoreactors, Applied Catalysis A: General 610 (2021) 117961.